Check for updates

Seasonally varying highway de-icing agent contamination in a groundwater plume from an infiltration basin

David W. Ostendorf, Richard N. Palmer and Erich S. Hinlein

ABSTRACT

This research documents the seasonal variation of de-icing agent contamination by measuring the specific conductivity of runoff and groundwater from an infiltration basin that serves a highway drainage system in southeast Massachusetts. The order of magnitude of the winter maxima of the runoff and groundwater specific conductivities over a 9 year period of record is 10 mS cm^{-1}. The groundwater specific conductivity decreases by 1–2 orders of magnitude to its fall minimum, which is an order of magnitude higher than the fall minimum of the runoff. This warm weather source behaviour implies slow, seasonal dissolution of de-icing agent solids deposited in the infiltration basin during the winter. A completely mixed reactor idealization of the basin models this postulate as a coupled balance of dissolved and solid de-icing agents. The data suggest that 13% of the de-icing agent solids applied to the highway deposits in the basin, where it dissolves into the infiltrating groundwater with a first order decay rate of 0.0035 day^{-1}.

Key words | groundwater pollution, infiltration, road salt, runoff, stormwater management

David W. Ostendorf (corresponding author)
Richard N. Palmer
Erich S. Hinlein
Civil and Environmental Engineering Department,
University of Massachusetts,
Amherst MA 01003,
USA
E-mail: *ostendorf@ecs.umass.edu*

NOMENCLATURE

A	surface area of de-icing agent solids deposited in the infiltration basin (m^2)
c	dissolved de-icing agent concentration (kg m^{-3})
c_{SAT}	saturated de-icing agent concentration (kg m^{-3})
D	hindered liquid diffusivity (m^2 s^{-1})
D_{FREE}	free liquid diffusivity (m^2 s^{-1})
F	flux of dissolved de-icing agent mass away from solid surface (kg s^{-1})
h	hydraulic head (m)
M	flux of suspended de-icing agent solids entering infiltration basin (kg s^{-1})
M^*	transformed flux of suspended de-icing agent solids entering infiltration basin (kg s^{-2})
n	porosity
p	Laplace transform variable (s^{-1})
Q	steady volumetric discharge of water through infiltration basin (m^3 s^{-1})
Q'	instantaneous volumetric discharge of water into infiltration basin (m^3 s^{-1})
R	radius of infiltration basin (m)
r	characteristic radius of de-icing agent solid granule (m)
S	mass of de-icing agent solids in the infiltration basin (kg)
S^*	transformed mass of de-icing agent solids in infiltration basin (kg s)
S_C	characteristic value of S (kg)
T	hydraulic residence time of infiltration basin (days)
t	time (s)
t_S	time of departure of reference frame from infiltration basin (s)
V	volume of water in the infiltration basin (m^3)
v	average linear velocity (m day^{-1})
x	distance along plume streamline (m)
z	near vertical position above bottom of groundwater plume (m)

doi: 10.2166/nh.2009.062

Downloaded from http://iwaponline.com/hr/article-pdf/40/6/520/372503/520.pdf
by guest

α vertical dispersivity (m)
δ root mean square of calibration error defined by Equation (3)
κ fraction of applied de-icing agents deposited in the infiltration basin
Λ ionic conductance of de-icing agents (mS m^3 (cm kg)$^{-1}$)
λ de-icing agent solid dissolution constant (days^{-1})
ρ_S de-icing agent solid density (kg m^{-3})
μ specific conductivity (S cm^{-1})
μ_O ambient specific conductivity (S cm^{-1})
μ_S specific conductivity at the infiltration basin at time t_S (S cm^{-1})
μ_S^* transformed specific conductivity at infiltration basin (S (cm s)$^{-1}$)
μ_W monthly average specific conductivity of runoff over the outlet weir (S cm^{-1})
μ_W' instantaneous specific conductivity of runoff over the outlet weir (S cm^{-1})
μ_W^* transformed specific conductivity of runoff over the outlet weir (S (cm s)$^{-1}$)
ζ diffusion gradient distance (m)

INTRODUCTION

Infiltration basins deliver wastewater treatment plant effluent (LeBlanc 1984), reused water (Houston *et al.* 1999), highway runoff (Dechesne *et al.* 2005) and other surface flows to the subsurface environment. As such, they may be regarded as anthropogenic unit processes at a hydrologic boundary, routing focused, contaminated surface water inputs to the underlying unconfined aquifer as infiltrating outputs. In this latter regard, basin effluents alter near-field advection by forming groundwater plumes that displace ambient streamlines (Ostendorf 1986). Highway infiltration basins also affect groundwater dispersion by adding storm scale aperiodicity (Ostendorf *et al.* 2008) to aquifer heterogeneity (Garabedian *et al.* 1991) as a source of average linear velocity fluctuations responsible for dispersion (Freeze & Cherry 1979).

Specific conductivity is well suited to document these groundwater transport mechanisms down-gradient of highway infiltration basins since it is conservative and easily measured. The analyte may be detected in surface water basin inputs by robust field sensors with field telemetry ideally suited for deployment at weirs or other control structures in highway drainage systems. These attributes are particularly attractive in cold climates, because specific conductivity is an excellent surrogate for major constituent concentrations of dissolved de-icing agents, on theoretical (Ostendorf *et al.* 2006) and experimental (Granato & Smith 1999) grounds. The agents are environmentally significant in their own right, due to potential impacts to stream (Rhodes *et al.* 2001; Kelly *et al.* 2008), river (Godwin *et al.* 2003), lake (Rosfjord *et al.* 2007), soil (Lofgren 2001) and groundwater quality (Bester *et al.* 2006; Howard & Maier 2007), as well as plant (Bryson & Barker 2002) and soil microbial (Gryndler *et al.* 2008) ecology. A thorough, documented, field-scale analysis of specific conductivity infiltration through a highway infiltration basin also sets the stage for future studies of reactive constituents such as trace metals or hydrocarbons. Infiltration basins are part of a best management practice portfolio for these sensitive stormwater analytes (Yu 1993), some of which have been considered at laboratory scale (Hipp *et al.* 2006; Hatt *et al.* 2008). A scale-up of these more fundamental studies from the laboratory to a highway and aquifer requires a well-characterized field site, particularly when a completely mixed reactor model (a unit process approach) is applied to stormwater remedial measures (Sansalone 2005). In particular, a temporally resolved, multiyear dataset elucidates hydrologic controls on the kinetics and fluxes that characterize the reactor, as is done in this study.

A completely mixed, flow through reactor (Tchobanoglous & Schroeder 1985) is used to describe an infiltration basin on State Route 25 in southeast Massachusetts with monthly specific conductivity observations over a nine year period of record (Figure 1). This reactor accepts input fluxes of runoff and de-icing agent solids from the drainage system of the highway, dissolves the solids as a chemical reaction, completely mixes the products and discharges output fluxes of groundwater of increased salinity to the aquifer. A simple advective dispersion model, calibrated with ample hydrogeologic data from the Plymouth-Carver aquifer, routes monitoring well samples back to the infiltration basin, quantifying the completely

Downloaded from http://iwaponline.com/hr/article-pdf/40/6/520/372503/520.pdf
by guest

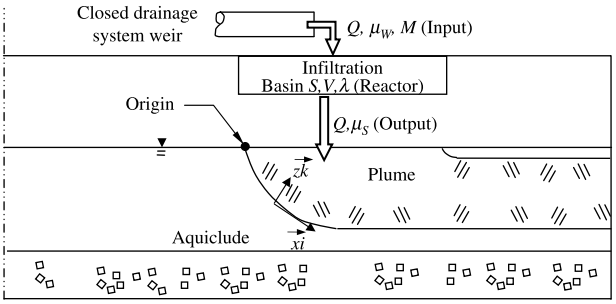

Figure 1 | Profile view of groundwater plume from a highway infiltration basin and schematic of the basin as a completely mixed reactor.

mixed reactor output. Monthly average discharge and specific conductivity of runoff are computed from values obtained from a drainage system weir, quantifying the reactor input. A consistent seasonal variation of unit process performance emerges: input specific conductivity declines by 2–3 orders of magnitude from a winter maximum to a fall minimum. The output specific conductivity declines by 1–2 orders of magnitude, so that the basin reaction generates specific conductivity during the summer and fall. A computed relationship between specific conductivity and dissolved de-icing agent concentrations casts this behaviour in terms of dissolved and solid agent partitions. De-icing agent application data and a coupled unit process model of dissolved and solid de-icing agents test the hypothesis that a fraction of the solids washes over the weir and deposits in the basin during the winter, then dissolves into the groundwater during the rest of the year.

SITE DESCRIPTION AND METHODS

Site description

Research was conducted at a well-characterized site in the Plymouth-Carver aquifer in southeast Massachusetts (Figure 2). The aquifer consists of glacial outwash deposits and recessional moraines (Hansen & Lapham 1992), and is 33 m thick in the site area (Meyer 1999) with a water table about 5 m below the ground surface. Grain size distributions and gravimetric moisture content analyses of split spoon samples from the site document a uniform medium sand with a 0.6 mm median grain size and a 30% porosity n (Meyer 1999). Pneumatic slug tests (Ostendorf *et al.* 2005)

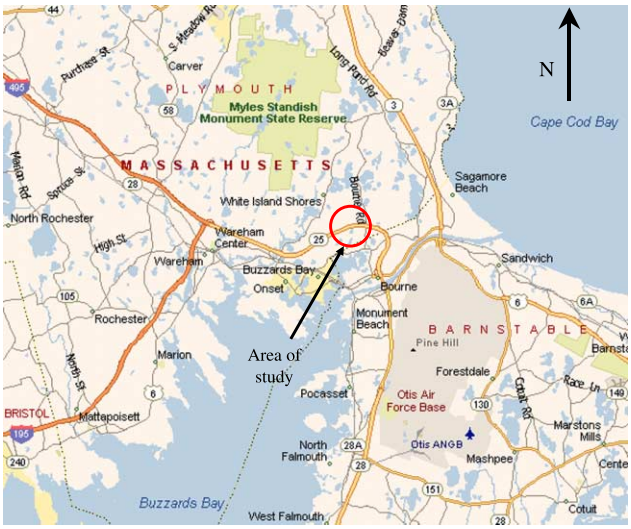

Figure 2 | Study area, along State Route 25 in southeast Massachusetts.

and pump tests (Ostendorf *et al.* 2007) calibrate a permeability of 10^{-10} m^2. Regional head data and isotopic tritium studies (Ostendorf *et al.* 2004) establish an ambient recharge rate of 2×10^{-8} m s^{-1}. The site features a groundwater plume from an infiltration basin receiving runoff from State Route 25. Ostendorf *et al.* (2008) calibrate a steady-state groundwater transport model of dissolved sodium, calcium, magnesium and chloride data at the site, and find an average linear velocity v of 0.95 m day^{-1} and a vertical dispersivity α of 34 cm. (Table 1 summarizes all adopted and calibrated parameter values.)

State Route 25 is a six-lane, divided, limited access highway that serves an average traffic volume of 55,000 vehicles per day (MHD 2008). The eastbound drainage system is closed, with kerbs, catch basins and pipes draining pavement 15.2 m wide, while the 15.2 m wide westbound pavement runoff flows to a 30 m wide median swale equipped with catch basins and pipes. The infiltration basin services 50,000 m^2, or 6.1 lane miles of pavement (Meyer 1999). Ostendorf *et al.* (2006) measured precipitation and runoff from 2000–2002 and found that 68% of the precipitation falling on the eastbound pavement drains to the basin, while 20% of the precipitation falling on the westbound pavement and median drains to the basin. The westbound lanes also feature a shoulder 3–5 m thick with a 20 cm thick loam cover layer and a capillary fringe, which

Downloaded from http://iwaponline.com/hr/article-pdf/40/6/520/372503/520.pdf
by guest

Table 1 | Adopted and calibrated parameter values

Symbol	Value	Source
c_{SAT}	348 kg m^{-3}	Ostendorf *et al.* (2006)
D	2.6 × 10^{-10} m^2 s^{-1}	Equation (7b)
D_{FREE}	1.3 × 10^{-9} m^2 s^{-1}	Logan (1999)
N	0.30	Meyer (1999)
Q	0.00173 m^3 s^{-1}	Ostendorf *et al.* (2008)
R	17 m	Ostendorf *et al.* (2007)
S_C	1,000 kg	Calibration*
T	1.8 days	Calibration*
V	269 m^3	Calibration*
v	0.95 m day^{-1}	Ostendorf *et al.* (2008)
α	0.35 m	Ostendorf *et al.* (2008)
κ	0.13	Calibration*
Λ	1.63 mS m^3 cm^{-1} kg^{-1}	Ostendorf *et al.* (2006)
λ	0.0035 days^{-1}	Calibration*
ρ_S	1790 kg m^{-3}	Ostendorf *et al.* (2006)
μ_O	80 μS cm^{-1}	Calibration*
ζ	16 cm	Calibration*

*Calibrated value established by this research.

receives windblown drift and, in winter, plowed precipitation. The lower fraction of westbound precipitation reaching the basin thus reflects evapotranspirative, infiltration and drift losses.

The pavement has been de-iced with salt (sodium chloride), premix (a blend of 80% salt by mass and 20% calcium chloride by mass) or calcium magnesium acetate since it opened in 1987. Ostendorf *et al.* (2006) analyzed MassHighway Department material expenditure reports from the storage facility serving State Route 25 for four de-icing seasons (November 1999 through April 2003) and found a 32% salt, 6% premix and 62% CMA distribution for their study period. They also computed an ionic conductance Λ of 1.63 mS m^3 cm^{-1} kg^{-1} relating specific conductivity μ to aqueous concentration c in runoff dissolving solid de-icing agents of this composition,

$$\mu = \Lambda c \tag{1}$$

along with values for the solid de-icing agent density ρ_S (1,790 kg m^{-3}) and the saturated concentration c_{SAT} (348 kg m^{-3}) of dissolved de-icing agent constituents. MassHighway has used a declining fraction of CMA since winter 2002/2003, stopping altogether before the onset of the winter 2006/2007 de-icing season. Figure 3 displays estimated monthly masses of de-icing agents applied to the 6.1 lane miles (50,000 m^2) of pavement that drain into the infiltration basin. A total mass of 6.7 × 10^5 kg has been applied over nine de-icing seasons, which corresponds to an estimated annual application rate of 7.7 kg per lane metre in the study area. The rate exceeds the value of 5.4 kg per lane metre for Maine (Mason *et al.* 1999), but is less than the 9.2 kg per lane metre value for New Hampshire and New York (TRB 1991) and the 12 kg per lane metre values reported for Sweden by Lofgren (2001) and southern Ontario by Labadia & Buttle (1996).

Groundwater methods and infiltration basin output

Surface and groundwater flow and specific conductivity, as well as precipitation, have been measured at the site from 2000 to the present through an instrumented drainage system outlet weir, monitoring wells and well clusters (Figure 4). The infiltration basin is south of the highway.

The wells and well clusters were of 5 cm diameter PVC construction, with respective screen lengths of 1.5 m and 30 cm. The wells and well clusters were installed through 10 cm diameter hollow stem augers, and native backfill was used along the casing and screen sections. Each well and well cluster was finished with a steel protective pipe with locking cap. The well clusters were screened at different elevations in separate, but closely spaced boreholes, and were intended to resolve the vertical concentration profile at a given horizontal location near the centreline of the

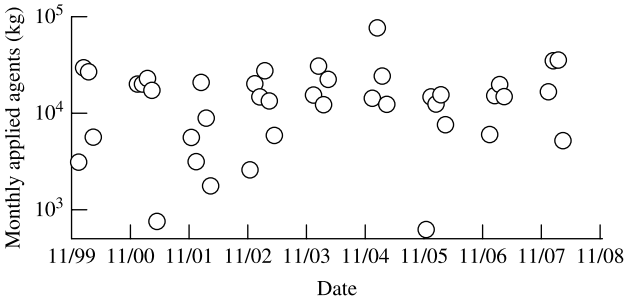

Figure 3 | Monthly de-icing agent masses (kg) applied to 6.1 lane miles (50,000 m^2) of pavement in study area.

Downloaded from http://iwaponline.com/hr/article-pdf/40/6/520/372503/520.pdf
by guest

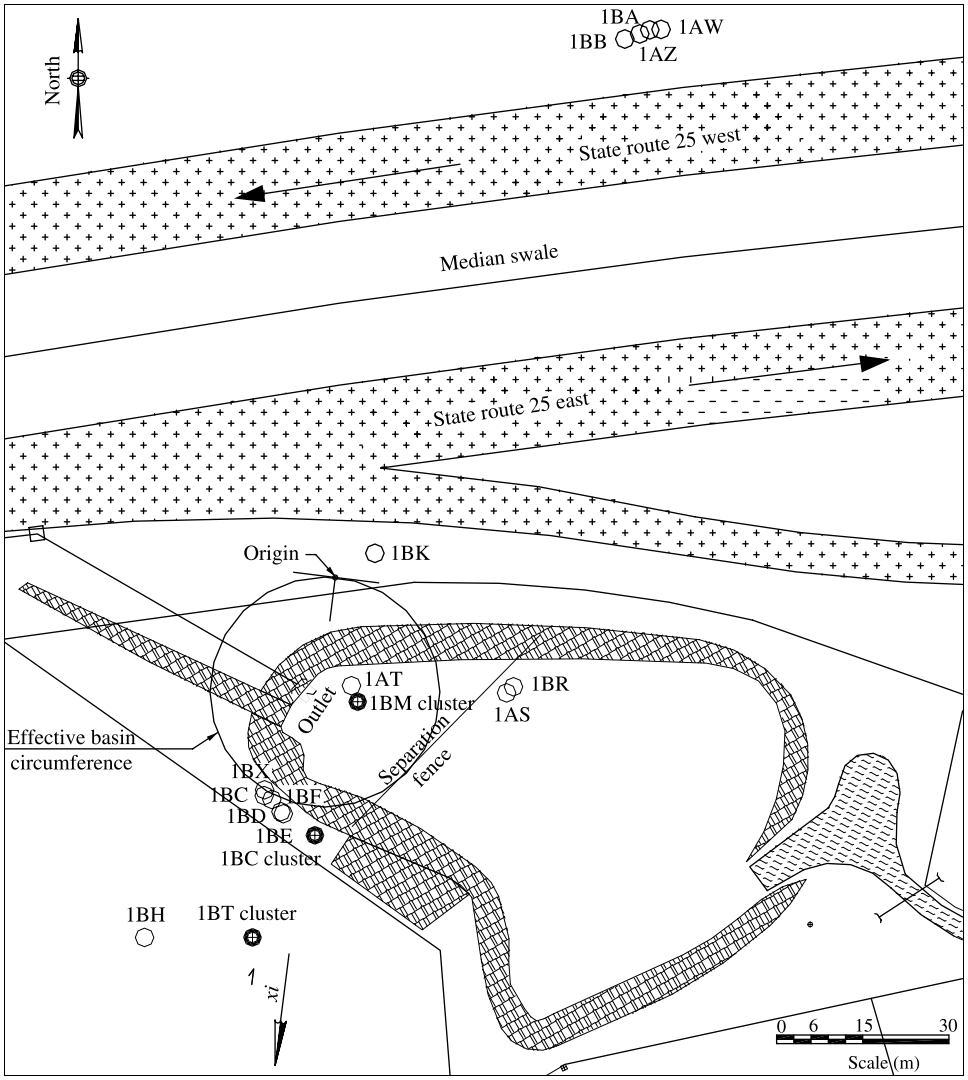

Figure 4 | Monitoring wells and well clusters at the State Route 25 field research site in southeast Massachusetts.

groundwater plume. The wells and well clusters are grouped in transects 28, 56 and 77 m downgradient from the upgradient boundary of the infiltration basin. The average linear velocity accordingly implies respective travel times of 32, 59 and 81 days, as noted in Table 2. The plume bottom descends about 8 m below the water table, in response to ambient groundwater flow and a calibrated average volumetric discharge Q of 0.00173 $m^3 s^{-1}$ through the basin.

Polypropylene tubing, Cam-Loc coupling, a one-way check valve (Brady Products, Inc; Clearwater, FL) and a model WX10 four stroke gasoline powered surface pump (Honda Corporation; Torrance, CA) were used to purge groundwater from each well (3 volumes) and well cluster (1.5 volumes). A sample was then collected in a 400 mL plastic beaker (Cole Parmer; Vernon, IL), where a model 30 handheld specific conductance meter (YSI; Yellow

Table 2 | Transects for control, monitoring wells and well clusters (Figure 4)

$t - t_s$ (days)	Wells	Well clusters
32	1AS, 1AT, 1BR	1BM, 8 depths
59	1BC, 1BD, 1BE, 1BF, 1BX	1BC, 7 depths
81	1BH	1BT, 8 depths
Control	1AW, 1AZ, 1BA, 1BB, 1BK	

Downloaded from http://iwaponline.com/hr/article-pdf/40/6/520/372503/520.pdf
by guest

Springs, OH) was used to measure groundwater specific conductivity. Monthly groundwater specific conductivity data extend from March 2000 through June 2008.

Monitoring wells AW, AZ, BA, BB and BK are upgradient of the groundwater plume, and form a control transect across the depth of the Aquifer. The shallower wells receive plowed precipitation, drift and open drainage from the westbound breakdown lane. Figure 5 displays average specific conductivity data for the control transect, which calibrates an ambient value μ_O of 80 μS cm^{-1}.

The symbols in Figure 6 are typical data. Since all transects were sampled on the same day (March 30, 2000), the furthest transect (Figure 6(c)) represents the earliest conditions at the infiltration basin. Specific conductivity increases with elevation at all three transects. The relatively low observations at the 81 day transect suggest that de-icing agent contamination for the 1999/2000 de-icing season had not arrived by March 30, 2000 while the higher values at the 32 and 59 day transects reflect arrival of contamination. This is qualitatively consistent with the travel times, in the sense that transect data reflect prior conditions at the infiltration basin. In this regard, the curves in Figure 6 are predictions (Equation (2a)) of the specific conductivity observed at time t and elevation z above the bottom of the plume:

$$\mu = \mu_O + \frac{\mu_S - \mu_O}{2}\left\{1 + \mathrm{erf}\left[\frac{z}{2\sqrt{\alpha v(t - t_S)}}\right]\right\} \quad (2a)$$

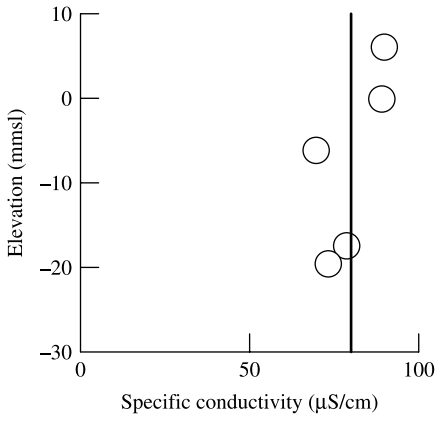

Figure 5 | Observed (symbols) and regressed (line) ambient specific conductivity at control transect. The latter specifies $\mu_O = 80$ μS cm^{-1}.

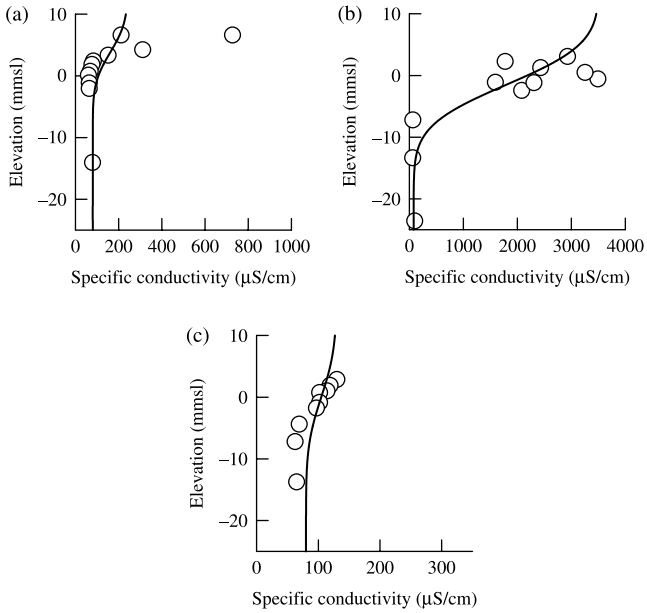

Figure 6 | Observed (symbols, for March 30, 2000) and calibrated (curves) specific conductivity at three transects downgradient of the infiltration basin: (a) 32 day travel time, (b) 59 day travel time and (c) 81 day travel time.

$$x = v(t - t_S) \quad (2b)$$

The source-specific conductivity μ_S corresponds to infiltrating groundwater leaving the basin at an earlier time t_S. The travel time $t - t_S$ appearing in Equation (2a) and (2b) and cited in Table 1 and Figure 6 refers to the frame of reference moving with the groundwater molecules along the bottom streamline of the groundwater plume at a constant average linear velocity v in the flow direction x (Figure 1). Equation (2a) describes the dispersive exchange of saline and ambient groundwater across the bottom of the plume, which progressively smears the vertical specific conductivity profile as the reference frame travels away from the infiltration basin. It is important to recognize that the specific conductivity is described in a moving frame, with negligible longitudinal dispersion, and advection is assumed uniform and steady. Indeed, Equation (2a) is a solution of the one-dimensional dispersion equation in an unbounded flow field (Fischer *et al.* 1979).

A nested Fibonacci search (Beveridge & Schechter 1970) calibrates μ_S and plume elevations for each monthly transect dataset in the present analysis. The search minimizes the root mean square of the calibration error δ,

Downloaded from http://iwaponline.com/hr/article-pdf/40/6/520/372503/520.pdf
by guest

defined by

$$\delta = \sqrt{\frac{1}{N}\sum_{N}\left(\frac{\mu(\text{measured}) - \mu(\text{predicted})}{\mu(\text{measured}) + \mu(\text{predicted})}\right)^2} \quad (3)$$

with specific conductivity predicted using Equation (2a), using the v and α values from prior investigations (Table 2). The error defined by Equation (3) is bound by unity and accordingly prevents extreme values from skewing the calibration. Figure 6 displays calibrations (as curves) for the March 30, 2000 data, which yield respective μ_S values of 241, 3,510 and 129 $\mu S\,cm^{-1}$ for the 32, 59 and 81 day transects. These calibrations in turn imply source times of 27 February 2000, 31 January 2000 and 9 January 2000, when the travel times are subtracted from the sample date. Similar calibrations, when performed for the period of record, yield a groundwater calibrated estimate of $\mu_S(t_S)$. Figure 7 displays, as symbols, the calibrated groundwater specific conductivities leaving the infiltration basin for the period of record.

Highway runoff methods and infiltration basin input

The three groundwater transects are downgradient of a groundwater recharge mound with an average radius R, 17 m in extent (Ostendorf *et al.* 2007). The mound forms about 1 m below the western boundary of the infiltration basin (Figure 4). The mound responds to stormwater runoff from the State Route 25 drainage system outlet, which flows over an instrumented, 90 degree V-notch weir installed at the end of a 92 cm diameter reinforced concrete pipe. The weir was equipped with a model 4320 bubbler flow meter (ISCO; Lincoln, NE) to measure the air pressure required to force air bubbles into water at a known displacement below the base of the weir, so that the hydraulic head h was known. This head was measured at 5 or 10 minute intervals from February 2000 through June 2008. A weir coefficient of 1.38 $m^{1/2}\,s^{-1}$ relates $h^{5/2}$ to the instantaneous volumetric water discharge over the weir Q' (White 2008). A model 600 multiparameter water quality monitor (YSI; Yellow Springs, OH) sampled temperature and weir specific (25°C) conductivity μ'_W at 5 or 10 minute intervals, with a range of 0–25 $mS\,cm^{-1}$ and an accuracy of 0.5%. Precipitation was also sampled on site at 5 or 10 minute intervals, using a model 647 L tipping bucket rain gauge (ISCO; Lincoln, NE). The site was powered with electricity from an adjacent utility line. The highway runoff data were telemetered to the laboratory computers of the University of Massachusetts Civil and Environmental Engineering Department, using dedicated cellular phone links.

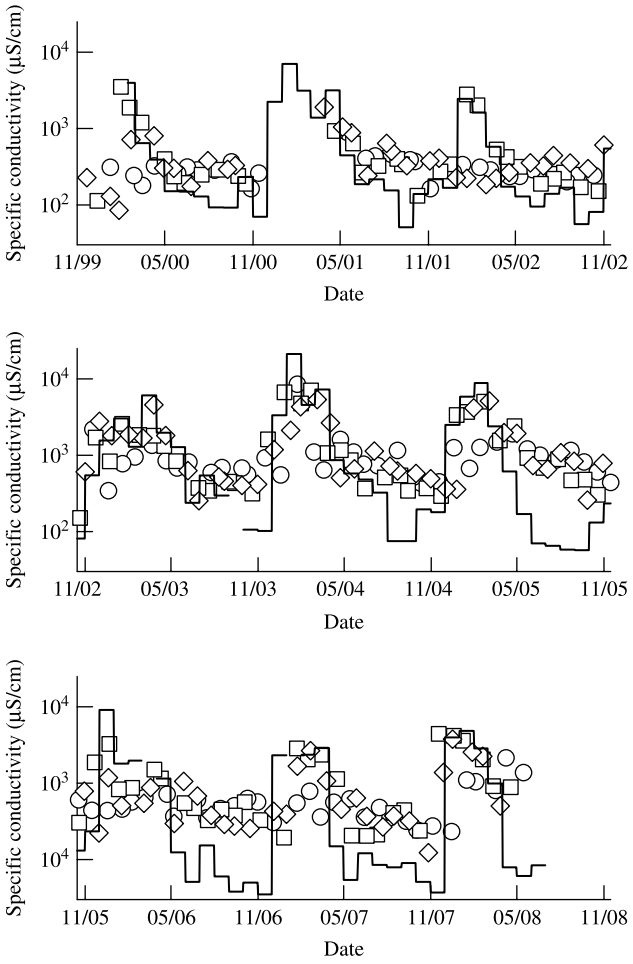

Figure 7 | Source groundwater (μ_S) specific conductivity implied by 32 (circles), 59 (squares) and 81 day (diamonds) monitoring well data, tracked back to infiltration basin with Equation (2a) and (2b). Monthly average runoff specific conductivity μ_W is shown as lines.

Figure 8 displays the hyetograph, hydrograph and specific conductivity pollutograph for March 2000. The latter varied from 0.056–19 $mS\,cm^{-1}$ during the month, with the high values associated with stagnant water behind the base of the weir between storms and the low values characterizing highway runoff flowing into the infiltration basin. Monthly average runoff concentrations μ_W are estimated as the ratio of the specific conductivity flux to

Downloaded from http://iwaponline.com/hr/article-pdf/40/6/520/372503/520.pdf
by guest

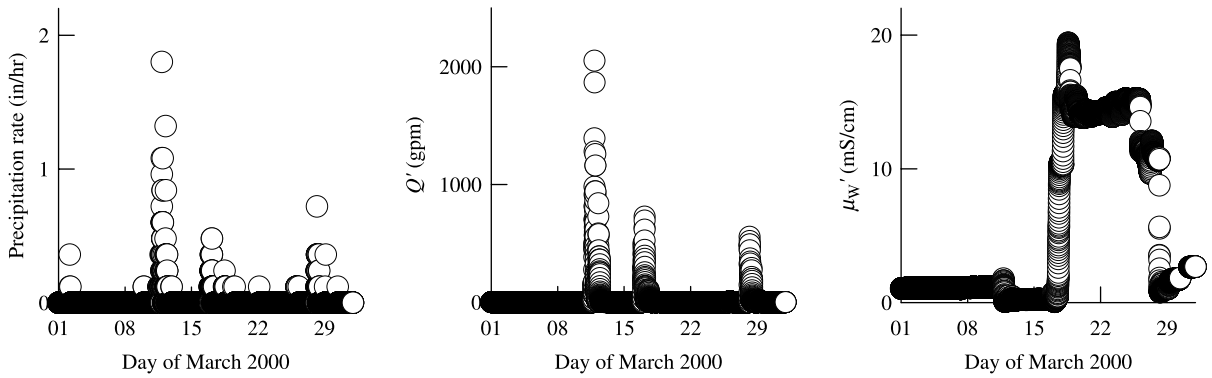

Figure 8 | Hyetograph, hydrograph and specific conductivity pollutograph at onsite rain gauge and instrumented weir for March 2000. Monthly average data appear as lines in Figure 7.

the water flux over the weir:

$$\mu_W = \frac{\int_{\text{month}} Q' \mu_W' \, dt_S}{\int_{\text{month}} Q' \, dt_S} \quad (4)$$

Equation (4) is evaluated numerically. The March 2000 data imply a μ_W of 643 $\mu S\,cm^{-1}$. Figure 7 displays (as lines) monthly average runoff specific conductivities for the period of record. The data acquisition failed during September 2003, March 2006 and January 2007, leaving three gaps in the runoff data base.

RESULTS AND DISCUSSION

Seasonal variation of specific conductivity of runoff entering the infiltration basin

Monthly average specific conductivity of the runoff range from 0.035 to 21.2 $mS\,cm^{-1}$, which corresponds to a concentration range of 0.021 to 13.0 kg dissolved de-icing agents per m^3 runoff when Equation (1) is considered. Broadly speaking, the runoff maxima occur in the winter at a 10 $mS\,cm^{-1}$ order of magnitude, and the specific conductivity decreases to fall minima that are 2–3 orders of magnitude below the winter levels.

Equation (1) and Figure 3 permit a comparison of the mass of de-icing agent solids applied annually to the pavement to the dissolved mass of de-icing agents flowing over the weir. Figure 3 suggests that the annual applications to the pavement served by the infiltration basin range from 4.0×10^4 to 1.3×10^5 kg of de-icing agents. The annual mass of dissolved agents in the runoff is computed by multiplying μ_W values by Q/Λ, then adding the monthly totals. These range from 1.7×10^4 to 1.1×10^5 kg dissolved de-icing agents per year entering the infiltration basin. Figure 9 displays both annual de-icing agent masses for the period of record; the dissolved de-icing agent mass is less than the applied mass in 8 of the 9 years reported. The average ratio of the dissolved to applied annual masses is 0.59. This value agrees with the findings of Ostendorf *et al.* (2006), who analyze applications, hydrographs and specific conductivity pollutographs for individual storms at the site and conclude that 55% of the applied de-icing agents dissolves into precipitation on the pavement.

Seasonal variation of specific conductivity in groundwater leaving the infiltration basin

Figure 7 plots (as symbols) the monthly specific conductivity in groundwater as it leaves the infiltration basin.

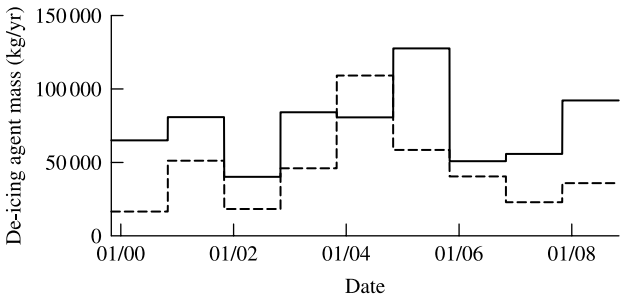

Figure 9 | Annual de-icing agent solid mass applied to pavement (solid lines) and dissolved de-icing agent mass discharged over the weir (dotted line).

Downloaded from http://iwaponline.com/hr/article-pdf/40/6/520/372503/520.pdf
by guest

The three transects imply consistent seasonal behaviour, with winter maxima of the order 10 mS cm^{-1}, similar to the runoff maxima. The groundwater specific conductivity does not drop as significantly as its runoff counterpart, however, decreasing 1–2 orders of magnitude to its fall minima. The 9 years of monthly data suggest that the infiltration basin adds specific conductivity to the water passing through during the summer and fall months, so that the exit infiltration is more saline than the incoming runoff. This may be explained by slow seasonal dissolution of de-icing agent solids that wash over the outlet weir and deposit in the basin during the de-icing season. A completely mixed reactor idealization of the basin models this hypothesis, subject to order of magnitude calibration by the data in Figure 7.

Seasonal dissolution of de-icing agent solids deposited in the infiltration basin

The Appendix couples seasonally varying completely mixed reactor models of specific conductivity and de-icing agent solids through the infiltration basin. A simple Laplace transform analysis suggests that the basin routes input dissolved and deposited solids with convolution integrals to the exit infiltration

$$\mu_S = \int_0^{t_S} \exp\left(-\frac{t_S-\tau}{T}\right)\left(\frac{\mu_W(\tau)}{T} - \frac{\Lambda M(\tau)}{V\left(\frac{1}{\lambda T}-1\right)}\right) + \frac{\Lambda M(\tau)}{V\left(\frac{1}{\lambda T}-1\right)}\exp[-\lambda(t_S-\tau)]d\tau \quad (5a)$$

$$T = \frac{Q}{V} \quad (5b)$$

with volume V of water in the infiltration basin and basin hydraulic residence time T. The basin radius and aquifer porosity values cited in Table 1 and a 1 m thickness from the ground surface to the groundwater mound imply a V of 272 m^3. This in turn yields a 1.8 day residence time, which is a rapid response compared to the seasonal variations implied by Figure 7. The basin therefore routes the input weir μ_W to the groundwater much faster than the slowly dissolving deposited solids, which are characterized by the first-order decay constant λ.

The observed monthly μ_W values in Figure 7 and a fraction κ of the monthly de-icing agent applications in Figure 3 drive the prediction (Equation (5a)) of μ_S, with the latter depositional flux M estimated by

$$M = \kappa \frac{\text{monthly application}}{\text{days in month}} \quad (6)$$

Adjacent monthly μ_W values are used to fill the three gaps in the runoff data base in order to generate a continuous prediction of μ_S. The μ_S values based on the monitoring well observations are construed as data and plotted in Figure 10, where the line in the figure is the calibrated Equation (5a). In the latter regard, a nested Fibonacci search through λ and κ minimizes δ at a value of 40%. This calibration accuracy implies order of

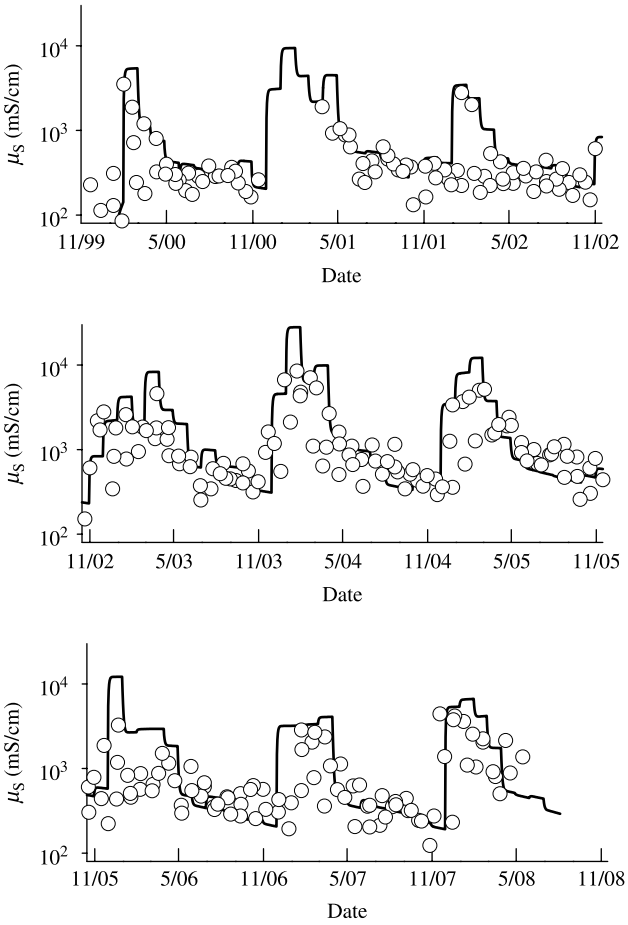

Figure 10 | Observed (all transects shown as circles) and predicted (line) source groundwater specific conductivity. Data are also plotted as three symbols in Figure 7.

Downloaded from http://iwaponline.com/hr/article-pdf/40/6/520/372503/520.pdf
by guest

magnitude agreement between observed and predicted μ_S values, which vary seasonally over 3 orders of magnitude and 9 de-icing seasons. The calibrated κ value of 0.13 suggests that an appreciable fraction of applied de-icing agents deposits in the infiltration basin. The deposited fraction is less than the 59% that dissolves on the pavement. The remaining 28% of the applied de-icing agents escapes the highway drainage system as plowed snow or windblown drift, consistent with the range of Blomqvist & Johansson (1999), who estimate that windblown drift and plowing deposits 20 to 60% of applied de-icing agents off the pavement of a Swedish highway.

The corresponding λ calibration (Figure 10) is 0.0035 days^{-1}: the deposited solids dissolve into draining runoff all year long. The physical basis of this calibrated decay constant can be examined by considering the dissolution at a smaller scale than that of the completely mixed reactor. Dissolved de-icing agent mass diffuses down a concentration gradient away from the surface area A of the solids in the basin, giving rise to a flux F approximated by

$$F = AD\frac{c_{SAT}}{\zeta} \tag{7a}$$

$$D = D_{FREE}n^{4/3} \tag{7b}$$

where liquid diffusivity D and dissolved concentration gradient c_{SAT}/ζ characterize the diffusion of contamination away from the surface of the de-icing agent solid. The concentration at the surface of the de-icing agent solid is saturated at a value c_{SAT}, and the liquid concentration decreases to a much lower value a distance ζ away from the solid surface. The tortuous paths through the soil of the infiltration basin hinder diffusion, so that D is less than the free diffusivity D_{FREE} of 1.2×10^{-9} m^2 s^{-1} cited by Logan (1999). A Millington (1959) model (Equation (7b)), together with the observed porosity lead to the 2.6×10^{-10} m^2 s^{-1} value used to interpret the first-order decay constant in terms of mass transport at a smaller scale.

The surface area A of all the solids in the basin may be related to their mass S by assuming spherical granules of characteristic radius r. This leads to first-order dissolution kinetics in the completely mixed reactor:

$$A = \frac{3S}{\rho_S r} \tag{8a}$$

$$F = \lambda S \tag{8b}$$

$$\lambda = \frac{3Dc_{SAT}}{\rho_S r\zeta} \tag{8c}$$

where ζ is taken as half the distance between adjacent de-icing agent solids in the basin, and so is related to a characteristic mass of solids S_C:

$$S_C = \rho_S\frac{4\pi r^3}{3}\left(\frac{R}{\zeta}\right)^2 \tag{9}$$

Equations (8c) and (9) are solved simultaneously for ζ with the result

$$\zeta = \left(\frac{3R}{\rho_S}\right)^{2/5}\left(\frac{4\pi}{S_C}\right)^{1/5}\left(\frac{Dc_{SAT}}{\lambda}\right)^{3/5} \tag{10}$$

A 1,000 kg S_C estimate, together with the parameter values cited in the nomenclature list, leads to a ζ value of 16 cm.

The seasonal persistence of specific conductivity in groundwater may be compared to the persistence of μ_W (Figure 7) in runoff, following the abrupt application of solid de-icing agents on the pavement (Figure 3). In the latter regard, Ostendorf *et al.* (2006) calibrate storm scale hydrograph and specific conductivity pollutograph models and a coupled de-icing agent solid model on the pavement with a first-order decay constant of 0.22 day^{-1}. This runoff delay, which is over an order of magnitude faster than the groundwater delay induced by the basin, is attributed to pavement texture, which shelters applied de-icing agent granules. Ostendorf *et al.* (2001, 2006) characterize dissolution kinetics of solid de-icing agents on the pavement in a fashion similar to Equation (10), and find a ζ of 7.6 cm. The longer gradient found in the present study implies slower dissolution kinetics and wider granule spacing in the basin.

CONCLUSIONS

Highway de-icing agents add appreciable ionic concentrations to surface runoff during winter months. This addition creates seasonally varying groundwater quality,

Downloaded from http://iwaponline.com/hr/article-pdf/40/6/520/372503/520.pdf
by guest

particularly when the runoff flows from a closed drainage system into an infiltration basin whose effluent forms a plume in the underlying aquifer. This seasonal variation is documented by measuring the specific conductivity of runoff and groundwater at a well-characterized plume from an infiltration basin that serves a highway drainage system in southeast Massachusetts. Monthly samples from three downgradient monitoring well and well cluster transects were used to calibrate specific conductivity values leaving the basin on the assumption of uniform advection, conservative contamination and vertical dispersion in the plume. These groundwater values are compared with monthly average specific conductivities measured in the runoff over the drainage system outlet weir from February 2000 to June 2008.

The order of magnitude of the winter maxima of the runoff and groundwater specific conductivities over the 9 year period of record is $10\,\mathrm{mS\,cm^{-1}}$. The groundwater specific conductivity decreases 1–2 orders of magnitude to its fall minimum, which is an order of magnitude higher than the fall minimum of the runoff: more dissolved contamination infiltrates into the aquifer than runs off into the basin during the summer and fall months. This behaviour is explained with a completely mixed, flow through reactor model of the infiltration basin that accepts de-icing agent solids and dissolved contamination from the outlet weir of the highway drainage system and routes dissolved contamination to the aquifer. The calibrated models suggest that 59% of the applied de-icing agent mass dissolves into precipitation on the pavement, while 13% of the applied de-icing agent mass is carried in suspension over the drainage weir and deposited in the infiltration basin. The deposited mass dissolves slowly in the infiltration basin, with a $0.0035\,\mathrm{day^{-1}}$ first-order decay constant.

ACKNOWLEDGEMENTS

The Massachusetts Highway Department funded this research under Interagency Service Agreement 38721. The views, opinions and findings contained in this paper are those of the authors, and do not necessarily reflect the official view or policies of MassHighway. This paper does not constitute a standard, specification or regulation.

REFERENCES

Abramowitz, M. & Stegun, I. A. 1972 *Handbook of Mathematical Functions*. National Bureau of Standards, Washington, DC.

Bester, M. L., Frind, E. O., Molson, J. W. & Rudolph, D. L. 2006 Numerical investigation of road salt impact on an urban wellfield. *Groundwater* **44**(2), 165–175.

Beveridge, G. S. G. & Schechter, R. S. 1970 *Optimization: Theory and Practice*. McGraw-Hill, New York, NY.

Blomqvist, G. & Johansson, E. L. 1999 Airborne spreading and deposition of deicing salt–a case study. *Sci. Total Environ.* **235**(1–3), 161–168.

Bryson, G. M. & Barker, A. V. 2002 Sodium accumulation in soils and plants along Massachusetts roadsides. *Commun. Soil Sci. Plan.* **33**(1–2), 67–78.

Dechesne, M., Barraud, S. & Bardin, J. P. 2005 Experimental assessment of stormwater infiltration basin evolution. *J. Environ. Eng.* **131**(7), 1090–1098.

Fischer, H. B., List, E. J., Koh, R. C. Y., Imberger, J. & Brooks, N. H. 1979 *Mixing in Inland and Coastal Waters*. Academic, New York, NY.

Freeze, R. A. & Cherry, J. A. 1979 *Groundwater*. Prentice-Hall, Englewood Cliffs, NJ.

Garabedian, S. P., LeBlanc, D. R., Gelhar, L. W. & Celia, M. A. 1991 Large scale natural gradient tracer test in sand and gravel, Cape Cod, MA 2. Analysis of spatial moments for a nonreactive tracer. *Water Resour. Res.* **27**(5), 911–924.

Godwin, K. S., Hafner, S. D. & Buff, M. F. 2003 Long term trends in sodium and chloride in the Mohawk River, New York: the effect of fifty years of road salt application. *Environ. Pollut.* **124**(2), 273–281.

Granato, G. E. & Smith, K. P. 1999 Estimating concentrations of road salt constituents in highway runoff from measurements of specific conductance. *WRIR 99-4077*. USGS, Northborough, MA.

Gryndler, M., Rohlenova, J., Kopecky, J. & Matucha, M. 2008 Chloride concentration affects soil microbial community. *Chemosphere* **71**(7), 1401–1408.

Hansen, B. P. & Lapham, W. W. 1992 Geohydrology and simulated groundwater flow, Plymouth-Carver Aquifer, southeastern Massachusetts. *WRIR 90-4024*. USGS, Marlborough, MA.

Hatt, B. E., Fletcher, T. D. & Deletic, A. 2008 Hydraulic and pollutant removal performance of fine media stormwater filtration systems. *Environ. Sci. Technol.* **42**(7), 2535–2541.

Hipp, J. A., Ogunseitan, O., Lejano, R. & Smith, C. S. 2006 Optimization of stormwater filtration at the urban/watershed interface. *Environ. Sci. Technol.* **40**(15), 4794–4801.

Houston, S. L., Duryea, P. D. & Hong, R. 1999 Infiltration considerations for groundwater recharge with waste effluent. *J. Irrig. Drain. Eng.* **125**(5), 264–272.

Howard, K. W. F. & Maier, H. 2007 Road deicing salt as a potential constraint on urban growth in the greater Toronto area, Canada. *J. Contam. Hydrol.* **91**(1–2), 146–170.

Downloaded from http://iwaponline.com/hr/article-pdf/40/6/520/372503/520.pdf
by guest

Kelly, V. R., Lovett, G. M., Weathers, K. C., Findlay, S. E. G., Strayer, D. L., Burns, D. J. & Likens, G. E. 2008 Long term sodium chloride retention in a rural watershed: legacy effects of road salt on streamwater concentration. *Environ. Sci. Technol.* **42**(2), 410–415.

Labadia, C. F. & Buttle, J. M. 1996 Road salt accumulation in highway snow banks and transport through the unsaturated zone of the Oak Ridges Moraine, southern Ontario. *Hydrol. Process.* **10**(12), 1575–1589.

LeBlanc, D. R. 1984 Sewage plume in a sand and gravel aquifer, Cape Cod, Massachusetts. *WSP 2218.* USGS, Washington, DC.

Lofgren, S. 2001 The chemical effects of deicing salt on soil and stream water of five catchments in southeast Sweden. *Water Air Soil Pollut.* **130**(1–4), 863–868.

Logan, B. E. 1999 *Environmental Transport Processes*. Wiley, New York, NY.

Mason, C. F., Norton, S. A., Fernandez, I. J. & Katz, L. E. 1999 Deconstruction of the chemical effects of road salt on stream water chemistry. *J. Environ. Qual.* **28**(1), 82–91.

Massachusetts Highway Department 2008 *Traffic volume counts*. www.state.ma.us./mhd/traffic

Meyer, M. M. 1999 *Fate and transport of deicing agent materials in an unconfined roadside aquifer*. PhD Thesis. University of Massachusetts, Amherst, MA.

Millington, R. J. 1959 Gas diffusion in porous media. *Science* **130**(3367), 100–102.

Ostendorf, D. W. 1986 Modeling contamination of shallow unconfined aquifers through infiltration beds. *Water Resour. Res.* **22**(3), 375–382.

Ostendorf, D. W., Peeling, D. C., Mitchell, T. J. & Pollock, S. J. 2001 Chloride persistence in a deiced access road drainage system. *J. Environ. Qual.* **30**(5), 1756–1770.

Ostendorf, D. W., Rees, P. L., Kelley, S. P. & Lutenegger, A. J. 2004 Steady, annual, and monthly recharge implied by deep unconfined aquifer flow. *J. Hydrol.* **290**(3–4), 259–274.

Ostendorf, D. W., DeGroot, D. J., Dunaj, P. J. & Jakubowski, J. 2005 A closed form slug test theory for high permeability aquifers. *Groundwater* **43**(1), 87–101.

Ostendorf, D. W., Hinlein, E. S., Ahlfeld, D. P. & DeJong, J. T. 2006 Calibrated models of deicing agent solids, pavement texture, and specific conductivity of highway runoff. *J. Environ. Eng.* **132**(12), 1562–1571.

Ostendorf, D. W., DeGroot, D. J. & Hinlein, E. S. 2007 Unconfined aquifer response to infiltration basins and shallow pump tests. *J. Hydrol.* **338**(1–2), 132–144.

Ostendorf, D. W., Rotaru, C. & Hinlein, E. S. 2008 Steady groundwater transport of highway deicing agent constituents from an infiltration basin. *J. Irrig. Drain. Eng.* **134**(5), 630–637.

Rhodes, A. L., Newton, R. M. & Pufall, A. 2001 Influences of land use on water quality of a diverse New England watershed. *Environ. Sci. Technol.* **35**(18), 3640–3645.

Rosfjord, C. H., Webster, K. E., Kahl, J. S., Norton, S. A., Fernandez, I. J. & Herlihy, A. T. 2007 Anthropogenically driven changes in chloride complicate interpretation of base cation trends in lakes recovering from acidic deposition. *Environ. Sci. Technol.* **41**(22), 7688–7693.

Sansalone, J. 2005 Perspective on the synthesis of unit operations and process concepts with hydrologic controls for rainfall–runoff. *J. Environ. Eng.* **131**(7), 995–997.

Tchobanoglous, G. & Schroeder, E. D. 1985 *Water Quality*. Addison-Wesley, Reading, MA.

Transportation Research Board 1991 Highway deicing comparing salt and calcium magnesium acetate. *Special Report No. 235.* NRC, Washington, DC.

White, F. M. 2008 *Fluid Mechanics*. McGraw-Hill, New York, NY.

Yu, S. L. 1993 Stormwater management for transportation facilities. *NCHRP Synthesis 174.* TRB, Washington, DC.

First received 24 July 2008; accepted in revised form 19 June 2009. Available online November 2009

Downloaded from http://iwaponline.com/hr/article-pdf/40/6/520/372503/520.pdf
by guest

APPENDIX: THE INFILTRATION BASIN AS A COMPLETELY MIXED REACTOR

Figure 1 schematizes the infiltration basin as a completely mixed reactor that receives runoff, specific conductivity and suspended de-icing agent solids from the drainage system outlet weir. The latter occurs during the de-icing season and deposits in the basin. The basin in turn discharges water and specific conductivity to the groundwater plume. The water flows steadily through the reactor, but the dissolved and solid de-icing agent concentrations vary seasonally.

The conservation of de-icing agent solids balances solids stored in the basin and dissolution of the solids:

$$\frac{\mathrm{d}S}{\mathrm{d}t_S} = M - F(\text{de}-\text{icing agent solids}) \tag{11}$$

The Laplace transform of Equations (8b) and (11) is taken and the initial mass of solids in the basin is neglected, with the result

$$S^* = \frac{M^*}{p+\lambda} \tag{12}$$

where S^* is transformed solids mass, M^* is transformed solids influx and p is the Laplace transform variable. Equation (12) yields a convolution integral solution (Abramowitz & Stegun 1972):

$$S = \int_0^{t_S} M(\tau)\exp[-\lambda(t_S-\tau)]\mathrm{d}\tau \tag{13}$$

The deposited de-icing agent solids dissolve into the water as it flows through the infiltration basin, and provide a source of specific conductivity to the solution. This dissolved water conservation equation balances storage, weir inflow, basin outflow and the dissolving de-icing agent solid source:

$$V\frac{\mathrm{d}\mu_S}{\mathrm{d}t_S} + Q\mu_S = Q\mu_W + \Lambda F \quad (\text{specific conductivity}) \tag{14}$$

The Laplace transform of Equations (8b) and (14), in view of Equations (5b) and (12), yields

$$\mu_S^* = \frac{\mu_W^*}{T\left(p+\frac{1}{T}\right)} + \frac{\Lambda\lambda M^*}{V(p+\lambda)\left(p+\frac{1}{T}\right)} \tag{15}$$

where μ_W^* and μ_S^* are transformed weir and source specific conductivity, respectively. The transform is inverted with convolution integrals, resulting in Equation (5a).

Downloaded from http://iwaponline.com/hr/article-pdf/40/6/520/372503/520.pdf
by guest